Author Manuscript
Author Manuscript
Author Manuscript
Author Manuscript

HHS Public Access
Author manuscript
*Neurobiol Dis*. Author manuscript; available in PMC 2021 December 22.

Published in final edited form as:
*Neurobiol Dis*. 2021 December ; 160: 105516. doi:10.1016/j.nbd.2021.105516.

# Targeting the VCP-binding motif of ataxin-3 improves phenotypes in *Drosophila* models of Spinocerebellar Ataxia Type 3

**Sean L. Johnson**[a], **Kozeta Libohova**[a], **Jessica R. Blount**[a], **Alyson L. Sujkowski**[a,b], **Matthew V. Prifti**[a], **Wei-Ling Tsou**[a], **Sokol V. Todi**[a,c,*]

[a]Department of Pharmacology, Wayne State University School of Medicine, Detroit, MI 48201, USA

[b]Department of Physiology, Wayne State University School of Medicine, Detroit, MI 48201, USA

[c]Department of Neurology, Wayne State University School of Medicine, Detroit, MI 48201, USA

## Abstract

Of the family of polyglutamine (polyQ) neurodegenerative diseases, Spinocerebellar Ataxia Type 3 (SCA3) is the most common. Like other polyQ diseases, SCA3 stems from abnormal expansions in the CAG triplet repeat of its disease gene resulting in elongated polyQ repeats within its protein, ataxin-3. Various ataxin-3 protein domains contribute to its toxicity, including the valosin-containing protein (VCP)-binding motif (VBM). We previously reported that VCP, a homo-hexameric protein, enhances pathogenic ataxin-3 aggregation and exacerbates its toxicity. These findings led us to explore the impact of targeting the SCA3 protein by utilizing a decoy protein comprising the N-terminus of VCP (N-VCP) that binds ataxin-3's VBM. The notion was that N-VCP would reduce binding of ataxin-3 to VCP, decreasing its aggregation and toxicity. We found that expression of N-VCP in *Drosophila melanogaster* models of SCA3 ameliorated various phenotypes, coincident with reduced ataxin-3 aggregation. This protective effect was specific to pathogenic ataxin-3 and depended on its VBM. Increasing the amount of N-VCP resulted in further phenotype improvement. Our work highlights the protective potential of targeting the VCP-ataxin-3 interaction in SCA3, a key finding in the search for therapeutic opportunities for this incurable disorder.

### Keywords

AAA ATPase; Ataxia; Ataxin-3; Deubiquitinase; *Drosophila* ; Machado-Joseph Disease; Neurodegeneration; Polyglutamine; Spinocerebellar Ataxia Type 3; VCP/p97

This is an open access article under the CC BY-NC-ND license (http://creativecommons.org/licenses/by-nc-nd/4.0/).

*Corresponding author at: 540 E. Canfield, Scott Hall Rm. 3108, Detroit, MI 48201, USA. stodi@wayne.edu (S.V. Todi).

Declaration of Competing Interest
The authors do not have anything to declare.

Appendix A. Supplementary data
Supplementary data to this article can be found online at https://doi.org/10.1016/j.nbd.2021.105516.

Author Manuscript Author Manuscript Author Manuscript Author Manuscript

## 1. Introduction

Spinocerebellar Ataxia Type 3 (SCA3, also known as Machado-Joseph Disease) is the most frequent, dominantly inherited ataxia in the world. Along with Huntington's disease, it is the predominant member of the family of polyglutamine (polyQ) neurodegenerative disorders that also includes SCAs 1, 2, 6, 7, and 17, Dentatorubral-pallidoluysian atrophy, and Kennedy's Disease (Coutinho and Andrade, 1978; Li et al., 2015; Matos et al., 2019; Paulson, 2012; Ranum et al., 1995; Rosenberg, 1992; Schöls et al., 2004). SCA3 is progressive, adult-onset and leads to neurodegeneration in cerebellar pathways, pontine and dentate nuclei, substantia nigra, globus pallidus, cranial motor nerve nuclei, anterior horn cells and peripheral nerves (Cancel et al., 1995; Dürr et al., 1996; Friedman, 2002; Friedman et al., 2003; Lin and Soong, 2002; Matos et al., 2019; Matsumura et al., 1996; Paulson, 2012; Rüb et al., 2004a; Rüb et al., 2003; Rüb et al., 2004b; Rüb et al., 2002a; Rüb et al., 2002b; Sasaki et al., 1995; Schöls et al., 1996; Sequeiros and Coutinho, 1993; Soong et al., 1997; Takiyama et al., 1994; Watanabe et al., 1998; Zhou et al., 1997). The underlying genetic defect in SCA3, like the other polyQ disorders, is the abnormal expansion of a CAG trinucleotide repeat that, once translated, results in polyQ protein aggregation and toxicity (Kawaguchi et al., 1994; Li et al., 2015; Matos et al., 2019; Paulson, 2012; Takiyama et al., 1993). In SCA3, CAG expansion occurs in the *ATXN3* gene (Kawaguchi et al., 1994; Li et al., 2015; Matos et al., 2019; Paulson, 2012; Takiyama et al., 1993), which encodes the 42 kD protein, ataxin-3 (Fig. 1A). The aberrant lengthening of the polyQ domain is a primary cause of all polyQ diseases, but each one is clinically distinct (Costa and Paulson, 2012; Klockgether et al., 2019; Lieberman et al., 2019; Nath and Lieberman, 2017; Pérez Ortiz and Orr, 2018; Todi et al., 2007b). This indicates that determinants of toxicity in these diseases are not only the polyQ repeats, but also the domains and interactions surrounding the expanded repeat, referred to as 'protein context'.

A body of work in polyQ diseases has highlighted a role for various non-polyQ regions and interactions in polyQ degeneration (Johnson et al., 2020; Matos et al., 2011; Nath and Lieberman, 2017; Pandey and Rajamma, 2018; Paulson et al., 2017; Pérez Ortiz and Orr, 2018; Todi et al., 2007a; Zoghbi and Orr, 2009). For ataxin-3, there are several domains that contribute to protein context and pathogenesis. As a deubiquitinating enzyme (DUB), the N-terminal half of ataxin-3 contains a ubiquitin-protease (Josephin) domain housing the catalytic triad that enables the protein to cleave isopeptide bonds (Costa and Paulson, 2012; Dantuma and Herzog, 2020; Winborn et al., 2008). The Josephin domain also contains two ubiquitin binding sites (UbS) that interact with ubiquitin (UbS1 and UbS2), or the proteasome-associated protein Rad23 (UbS2) (Costa and Paulson, 2012; Dantuma and Herzog, 2020; Nicastro et al., 2009; Nicastro et al., 2010). Downstream of the Josephin domain are two ubiquitin-interacting motifs (UIMs 1 and 2), a site that binds the AAA ATPase known as valosin-containing protein (VCP, or p97; this site is termed the VCP-binding motif or 'VBM'), and the polyQ domain (Costa and Paulson, 2012; Dantuma and Herzog, 2020; Todi et al., 2007b; Winborn et al., 2008). The C-terminus of ataxin-3, following the polyQ domain, commonly contains an additional UIM, although an isoform also exists that does not contain the third UIM (Costa and Paulson, 2012; Dantuma and Herzog, 2020).

Author Manuscript Author Manuscript Author Manuscript Author Manuscript

We recently showed that the VBM is a significant contributor to ataxin-3 pathogenicity (Ristic et al., 2018; Sutton et al., 2017). The VBM comprises the arginine-rich sequence 'RKRR' which, when mutated into the amino acid sequence 'HNHH', no longer binds VCP (Boeddrich et al., 2006). VCP is a ubiquitous, homo-hexameric AAA ATPase that is bound directly at its N-terminus by ataxin-3 through the VBM (Boeddrich et al., 2006; Buchberger et al., 2010) (Fig. 1A). VCP regulates the proteasomal degradation of various proteins (Buchberger et al., 2010; Dai et al., 1998; Kim et al., 2013; Meyer et al., 2012); however, mutations that disable binding of ataxin-3 to VCP do not impact ataxin-3 protein levels (Blount et al., 2014; Ristic et al., 2018; Sutton et al., 2017; Tsou et al., 2015b) or its subcellular distribution (Ristic et al., 2018).

Our previous work exploring the role of the ataxin-3-VCP interaction utilized *Drosophila melanogaster* models of SCA3 expressing full-length, human ataxin-3 with and without the mutation that prevents VCP-binding. Mutating the pathogenic ataxin-3 VBM improved fly motility and longevity compared to counterparts expressing pathogenic ataxin-3 Q80 with an intact VBM (Ristic et al., 2018). Biochemically, mutating ataxin-3's VBM or reducing the levels of VCP through RNA-interference did not reduce SCA3 protein levels, but decreased pathogenic ataxin-3 aggregation (Johnson et al., 2020; Ristic et al., 2018) – a critical observation given that, in our assays with pathogenic ataxin-3, its aggregation precedes toxicity (Johnson et al., 2019; Johnson et al., 2020; Ristic et al., 2018; Sutton et al., 2017). These and other findings led us to conclude that pathogenic ataxin-3 with a mutated VBM is less aggregation-prone and less toxic. They also described an important role for VCP in determining ataxin-3 toxicity, suggesting a model where multiple ataxin-3 proteins bind individual VCPs in a single hexamer (Ristic et al., 2018). These interactions may bring pathogenic ataxin-3 proteins into closer proximity, increasing their chances of interaction and aggregation – i.e., VCP seeds the aggregation of ataxin-3, exacerbating its toxicity.

These prior findings prompted the question that we tackle in this study: might we reduce the toxicity of pathogenic ataxin-3 by disrupting its interaction with VCP through a 'decoy' approach targeting the VBM? We utilized a truncated protein that consists of the VCP N-terminus (amino acids 1–199), denoted at 'N-VCP', that binds ataxin-3 (Boeddrich et al., 2006), but cannot hexamerize (DeLaBarre et al., 2006; Kobayashi et al., 2002; Mori-Konya et al., 2009; Wang et al., 2003) (Fig. 1A). As VCP is a critical protein, whereas ataxin-3 is dispensable in mice (Costa and Paulson, 2012; Matos et al., 2011; Schmitt et al., 2007; Switonski et al., 2011; Zeng et al., 2013), we reasoned that it would be more practical to target ataxin-3 rather than VCP so as not to impede VCP functions while still hindering the interaction of interest. As shown in the results, we find that N-VCP ameliorates the toxicity of pathogenic ataxin-3 at all stages and in all tissues tested in the fruit fly. The protective effect of N-VCP is specific to pathogenic ataxin-3 and is dependent on its VBM. Also, the beneficial effect of the N-VCP truncated protein is enhanced by increasing its levels. This work expands on our understanding of this critical protein-protein interaction in SCA3 and highlights the disruption of ataxin-3's interaction with VCP as a potential therapeutic strategy for this neurodegenerative disease.

Author Manuscript Author Manuscript Author Manuscript Author Manuscript

## 2. Materials and methods

### 2.1. Antibodies

Anti-Ataxin-3: mouse monoclonal 1H9, 1:500–1000; Millipore; rabbit polyclonal, 1:15000 (Paulson et al., 1997). Anti-HA: rabbit monoclonal, 1:500–1000; Cell Signaling Technology. Anti-Myc: mouse monoclonal 9E10, 1:500–1000; Santa Cruz Biotechnology. Anti-VCP: rabbit monoclonal, 1:500–1:1000; Cell Signaling Technology. Peroxidase-conjugated secondary antibodies: goat anti-mouse and goat anti-rabbit, 1:5000; Jackson ImmunoResearch.

### 2.2. Construct design

Human ataxin-3 cDNAs were based on sequences from previous publications and include either 77 or 80Q (Berke et al., 2005; Blount et al., 2012; Harris et al., 2010; Johnson et al., 2019; Johnson et al., 2020; Nicastro et al., 2009; Nicastro et al., 2010; Ristic et al., 2018; Sutton et al., 2017; Todi et al., 2009; Tsou et al., 2015b; Winborn et al., 2008). We used the company Genscript (genscript.com) to synthesize the VCP N-terminus cDNA as well as full-length fly VCP. An N-terminal Myc tag-encoding sequence was added immediately preceding the VCP start codon. Transgenes were sub-cloned into pWalium-10.moe. Transgenic fly lines were generated via phiC31 integration into either attP2 (ataxin-3) on chromosome 3 or attP40 (N-VCP, VCP) on chromosome 2 (Blount et al., 2012; Blount et al., 2020; Fish et al., 2007; Groth et al., 2004; Johnson et al., 2019; Johnson et al., 2020; Ristic et al., 2018; Sutton et al., 2017; Tsou et al., 2015b; Tsou et al., 2016). Each insertion was confirmed and validated by PCR, genomic sequencing, and Western blotting, using procedures described in previous work (Blount et al., 2018; Johnson et al., 2019; Johnson et al., 2020; Ristic et al., 2018; Sutton et al., 2017; Tsou et al., 2015b; Tsou et al., 2016).

### 2.3. Drosophila husbandry

Common fly lines were obtained from the Bloomington *Drosophila* Stock Center: GMR-Gal4 (#8121), the isogenic host strain attP2 (#36303), and the isogenic host strain attP40 (#36304). FlyORF was used to obtain an additional fly VCP line (TER94, #F001765) used in Supplemental Fig. 4. The following stocks were gifts: sqh-Gal4 (Dr. Daniel P. Kiehart, Duke University), elav-Gal4-GS (Dr. R. J. Wessells, Wayne State University), elav-Gal4 and repo-Gal4 (Dr. Daniel F. Eberl, University of Iowa). Unless otherwise stated in the figure legends and text, all flies were heterozygous for driver and transgene(s). Whenever ataxin-3 and VCP or N-VCP were co-expressed, their expression was driven by the same Gal4 driver, in the same tissues, and at the same developmental and/or adult time points. All crosses were conducted at 25 °C in diurnal environments with 12 h light/dark cycles and on conventional cornmeal or RU486-containing media, and all resulting offspring were maintained in the same conditions (Johnson et al., 2019; Johnson et al., 2020; Sujkowski et al., 2015).

### 2.4. Drosophila examinations

Longevity experiments were performed with adults collected on the day of eclosion and deaths were recorded daily. Flies were observed from the embryo stage through eclosion

Author Manuscript Author Manuscript Author Manuscript Author Manuscript

and deaths at each developmental stage were recorded daily, as summarized in figures. Fly eye scoring was conducted using numerical scales where a higher score indicates a worse phenotype. Breakdowns of the phenotypes for each scale are shown in respective figures and legends. Motility tests were conducted using the negative geotaxis assay, where fifteen flies per vial were tapped to the bottom of the vial and the total number of flies reaching the top was recorded at 5, 15 and 30s and expressed as percent of total flies. Flies that reached the top were scored only once.

### 2.5. Western blotting and quantification

Depending on the experiment 3 or 5 flies, or 10 dissected adult heads (unless otherwise specified), per group were homogenized in boiling fly lysis buffer (50 mM Tris pH 6.8, 2% SDS, 10% glycerol, 100 mM dithiothreitol), sonicated, boiled for 10 min, and then centrifuged at 13300 ×*g* at room temperature for 10 min. Western blots were developed with either PXi 4 (Syngene) or ChemiDoc (Bio-Rad) and quantified with GeneSys (Syngene) or ImageLab (Bio-Rad), respectively. To conduct direct blue stains, the PVDF membranes were submerged for 10 min in 0.008% Direct Blue 71 (Sigma-Aldrich) in 40% ethanol and 10% acetic acid, rinsed in 40% ethanol/10% acetic acid, air dried, and imaged.

### 2.6. Filter-trap assay

For each group, 10 dissected fly heads were homogenized in 200 μL NETN buffer (50 mM Tris, pH 7.5, 150 mM NaCl, 0.5% Nonidet P-40) supplemented with protease inhibitor cocktail (PI; S-8820, Sigma-Aldrich). Following homogenization, lysates were diluted with 200 μL PBS containing 0.5% SDS, sonicated briefly, then centrifuged at 4500 ×*g* for 1 min at room temperature. 100 μL of supernatant was then diluted further with 400 μL PBS. Depending on the experimental setup, either 20 or 30 μL of each sample were filter-vacuumed using a Bio-Dot apparatus (Bio-Rad) through a 0.45 μm nitrocellulose membrane (Schleicher and Schuell) that was pre-incubated and rinsed with 0.1% SDS in PBS. Following filter-vacuuming of the samples, the membrane was rinsed twice with 0.1% SDS in PBS, incubated with primary and secondary antibodies, and analyzed by Western blotting.

### 2.7. Co-immunopurifications

40–80 dissected fly heads or 20 whole flies, depending on the experiment, were lysed in NETN/PBS (50%/50%) + PI, tumbled at 4 °C for 30 min, then centrifuged at 4 °C for 5 min at 5000 ×g. The supernatant was incubated with bead bound antibody (either Myc- or HA-tagged; Fisher Scientific) for 2 h. Beads were then rinsed 1–3× with NETN/PBS + PI (depending on experiment) followed by elution of bead-bound complexes by boiling in 2% SDS buffer with 100 μM DTT.

### 2.8. Statistical analyses

Statistical tests used are noted in the figure legends. Prism 8 (GraphPad) was used for log-rank tests with Holm-Bonferroni adjustments, Repeated-measures and ordinary one-way ANOVA with Tukey's multiple comparisons test, Mann-Whitney tests, and Kruskal-Wallis tests. Additional data collection and organization, as well as student's *t*-tests, were

Author Manuscript Author Manuscript Author Manuscript Author Manuscript

performed in Excel (Microsoft), or Numbers (Apple). *p*-values were calculated by the software used for analyses and indicated in the corresponding figures and legends, alongside the number of biological replicates.

## 3. Results

### 3.1. N-VCP is non-toxic to Drosophila and interacts with pathogenic ataxin-3

The N-terminus of VCP is sufficient and necessary to bind ataxin-3 at its VBM in vitro (Boeddrich et al., 2006). The N-VCP truncated protein that we utilize here consists of amino acids 1–199 of VCP (Fig. 1A). An N-terminal Myc-tag was added to N-VCP and expression in *Drosophila* was confirmed with a ubiquitous Gal4 driver (spaghetti squash, sqh, Fig. 1B; additional examples are in Figs. 3, 4, 6, 8). Here, as in previous studies, we take advantage of *Drosophila* genetics and the Gal4-UAS binary system of expression (Blount et al., 2018; Blount et al., 2014; Burr et al., 2014; Johnson et al., 2019; Johnson et al., 2020; Ristic et al., 2018; Sutton et al., 2017; Tsou et al., 2015a; Tsou et al., 2015b; Tsou et al., 2016). Each Gal4 driver expresses ataxin-3 and N-VCP in a specific tissue either individually or together, as indicated in the text and figures. In longevity assays, N-VCP expression is non-toxic whether expressed ubiquitously (sqh-Gal4) or pan-neuronally (elav-Gal4; Fig. 1C,D). This was also validated in motility assays, where the pan-neuronal expression of N-VCP did not impact fly motility compared to controls that contained the driver but did not express N-VCP (Supplemental Fig. 1). Co-immunopurification assays (co-IPs) conducted in flies pan-neuronally co-expressing N-VCP and full-length, human, pathogenic (80Q) ataxin-3 confirmed that N-VCP interacts with ataxin-3 (Fig. 1E), setting the stage for an investigation into N-VCP's impact on pathogenic ataxin-3 toxicity in the fly.

### 3.2. Presence of N-VCP is ameliorative in SCA3 models of different toxicity

The *Drosophila* lines modeling SCA3 were designed in two stages. While both express full-length, UIM3-containing, human ataxin-3 protein with patient-range repeats of 77–80Q, one of the lines is designated as 'stronger' (Q80) and the other as 'weaker' (Q77), based on their comparative toxicity to flies. The difference in lethality is due to the 'stronger' line containing an ataxin-3 transgene with an optimized Kozak sequence that results in higher ataxin-3 protein levels (Johnson et al., 2019). However, it is important to note that beyond the differences in toxicity, the 'stronger' and 'weaker' transgenes are inserted into the same chromosomal site in *Drosophila* (attP2 on chromosome 3) and are on the same genetic background (w1118; Fig. 2A). Expression was tested in various tissues to obtain a comprehensive understanding of the impact of N-VCP on ataxin-3-related toxicity: ubiquitous expression because ataxin-3 is expressed everywhere; pan-neuronal expression because SCA3 is primarily a neuronal disease; adult-only, pan-neuronal expression because SCA3 is adult-onset; and expression in fly eyes to observe more changes across phenotypes over time.

We began our investigations by examining the impact of N-VCP expression on the 'weaker' SCA3 line. As summarized in Fig. 2B, ubiquitous co-expression of pathogenic ataxin-3 and N-VCP led to reduced lethality at various developmental stages: a significantly smaller proportion of developing flies died in pupal, pharate, and eclosing stages in the presence

Author Manuscript Author Manuscript Author Manuscript Author Manuscript

of N-VCP than in its absence when pathogenic ataxin-3 was co-expressed in all tissues. Concomitantly, more adult flies successfully eclosed from the pupal case and were tracked for longevity in the presence of N-VCP than in its absence (Fig. 2C).

Perhaps counterintuitively at first, most 'weaker' SCA3 adults died earlier with co-expression of N-VCP (Fig. 2C and Supplemental Fig. 2). We believe this is due to the fact that only a small portion of SCA3 flies eclose as adults in the absence of N-VCP and that they represent the strongest among that population of developing flies. While only the presumed healthiest flies expressing the 'weaker' ataxin-3 alone emerged as adults – ~11% of the total developing flies – ~70% of flies co-expressing ataxin-3 and N-VCP emerged as adults. Among the latter, the longest-surviving adults lived markedly longer than flies without N-VCP (Supplemental Fig. 2), nearly as long as controls that do not express pathogenic ataxin-3 or N-VCP (Fig. 2C). Expression of the 'weaker' SCA3 line pan-neuronally at all times (Fig. 2D) or only in adults (Fig. 2E) also resulted in less severe toxicity in the presence of N-VCP. Collectively, these findings indicate that N-VCP suppresses lethality in the 'weaker' SCA3 line.

Encouraged by the reduction in lethality in the presence of N-VCP with the 'weaker' SCA3 model, we next tested if these results persist in the 'stronger' line. Similar to what we observed with the 'weaker' model, ubiquitous N-VCP co-expression alongside the 'stronger' SCA3 transgene significantly decreased the proportion of developmental deaths and was critical in allowing pupae to enter the pharate adult stage (Fig. 3A). Among flies that ubiquitously expressed pathogenic ataxin-3 Q80 alone, over 95% died as pupae, with only a small portion of the remaining developing flies advancing to the pharate adult stage (Fig. 3A). Conversely, flies co-expressing N-VCP and ataxin-3 Q80 commonly reached the pharate adult stage prior to death (~79%), and a small percentage initiated the eclosing process from the pupal case, but died before emerging successfully (Fig. 3A).

To allow for more longitudinal studies in adult flies and to mimic the adult-onset characteristic of SCA3, an inducible pan-neuronal driver was once again employed to express the 'stronger' ataxin-3 transgene with and without N-VCP in adult flies only, with expression starting on day 1 after emergence from the pupal case. N-VCP co-expression significantly increased fly longevity (Fig. 3B), mirroring what we observed with the 'weaker' SCA3 model (Fig. 2E).

As will be detailed further below, reduced toxicity from N-VCP was not due to lack of pathogenic ataxin-3 in the presence of N-VCP. Pathogenic ataxin-3 is still abundantly present when co-expressed with N-VCP (Fig. 3C). Additionally, co-expression of N-VCP alongside pathogenic ataxin-3 leads to reduced levels of endogenous VCP coprecipitating with the SCA3 protein (Fig. 3D; please see Fig. 8C for additional data and quantitative information).

We also performed motility studies in flies with the inducible pan-neuronal driver (Supplemental Fig. 3). Although early in life flies expressing the 'stronger' pathogenic ataxin-3 with N-VCP showed a slight improvement compared to those expressing ataxin-3 alone, they did not reach the motility level of control flies that did not express pathogenic

Author Manuscript Author Manuscript Author Manuscript Author Manuscript

ataxin-3 or N-VCP; also, the improvement was no longer apparent by the third week (Supplemental Fig. 3). Collectively these results indicate that the presence of N-VCP is effective in reducing SCA3 toxicity in *Drosophila*.

As an additional counterpoint to the protective role from N-VCP that we observed so far, we tested whether increased expression of full-length VCP has the opposite effect, as predicted by our prior work (Ristic et al., 2018). We generated flies that contain either one or two genetic copies of fly VCP and compared lethalities when co-expressed with either the 'weaker' or 'stronger' SCA3 model. As shown in Supplemental Fig. 4, VCP over-expression led to worse developmental outcomes that were exacerbated by increased genetic copies of VCP in both SCA3 models, providing additional support for our model that VCP impacts ataxin-3 toxicity.

### 3.3. The effects of N-VCP are specific to ataxin-3 with an intact VBM

We have, so far, observed a protective effect from N-VCP on ataxin-3-dependent toxicity (Figs. 2, 3). Our model posits that this effect centers on the VBM of ataxin-3. To ensure that indeed the VBM of ataxin-3 is required for the protective role of N-VCP, we examined its ability to impact toxicity caused by pathogenic ataxin-3 with a mutated VBM, which does not interact with VCP in vitro, in mammalian cells or in flies (Ristic et al., 2018). This VBM-mutated line of SCA3 is isogenic to the SCA3 'weaker' line introduced above (Ristic et al., 2018) and was expressed in flies with or without co-expression of N-VCP.

In this modified ataxin-3 line, the VBM sequence 'RKRR' was mutated into 'HNHH'. Flies expressing pathogenic ataxin-3 with mutated VBM show reduced degenerative phenotypes and this version of ataxin-3 is less aggregation-prone than the SCA3 protein with a functional VBM (Ristic et al., 2018). Through co-IPs, we confirmed that N-VCP requires a functional VBM on pathogenic ataxin-3 to interact with it specifically (Fig. 4A). Survival analyses from these flies showed that mutating the VBM of ataxin-3 eliminates the toxicity-mitigating effect of N-VCP pan-neuronally. In fact, N-VCP exacerbated lethality when it was co-expressed ubiquitously with pathogenic ataxin-3 that it can no longer bind (Fig. 4B and C).

To further clarify that the benefits of N-VCP co-expression are specific to ataxin-3, we conducted experiments examining the potential impact of N-VCP on a pathogenic protein linked to a different polyQ disorder, SCA6. α1ACT is a polyQ-containing transcription factor that is generated from the bicistronic mRNA of the *CACNA1A* gene, which causes SCA6 (Du et al., 2013; Lieberman et al., 2019). We selected this protein because it is not reported to have any interaction with VCP, a statement that we would not be as confident in making with proteins related to other polyQ diseases, like SCA7 and SCA1 (Franceschini et al., 2016; Szklarczyk et al., 2019; Szklarczyk et al., 2017). The interaction of VCP with other polyQ disease proteins, including SCA1 and SCA7, has been confirmed by experimental evidence, as indicated in previous work and the STRING database (Franceschini et al., 2016; Fujita et al., 2013; Szklarczyk et al., 2019).

We expressed human α1ACT with a pathogenic 70Q repeat in flies with and without N-VCP, either ubiquitously or pan-neuronally, throughout development and in adults.

Author Manuscript Author Manuscript Author Manuscript Author Manuscript

Ubiquitously expressed α1ACT (Q70) by itself was toxic: most developing flies died as pharate adults, and the handful that emerged as adults died by day 16 (Fig. 4D). In this SCA6 model, ubiquitous co-expression of N-VCP did not improve the phenotype: all flies died as pharate adults, and no adults emerged (Fig. 4D). Pan-neuronal expression of α1ACT(Q70) was less toxic than ubiquitous expression (Fig. 4E), as also shown before (Tsou et al., 2015a; Tsou et al., 2016). Co-expression of N-VCP did not provide a detectable benefit compared to flies expressing α1ACT(Q70) alone (Fig. 4D, E). We conclude that the reduced toxicity of pathogenic ataxin-3 observed in the presence of N-VCP is specific to ataxin-3 with a functional VBM.

### 3.4. N-VCP alleviates SCA3 phenotype in fly eyes

To expand on our observations, we shifted our focus to a SCA3 model specific to the fly eye. We previously utilized similar models to observe the phenotypic deterioration that occurs with pathogenic ataxin-3 expression, as well as to perform screens of various molecules and genetic modifications that may ameliorate SCA3 (Ashraf et al., 2020; Johnson et al., 2020). Observation of the eye allows for the detection of more subtle changes among groups of flies that might go undetected in other expression patterns. We thought it reasonable to use the fly eye to further examine the impact of N-VCP in flies that co-express human, pathogenic ataxin-3. In models expressing the ‘stronger’ ataxin-3 in fly eyes (GMR-Gal4), the eyes appear normal (wild-type) at eclosion and worsen continually over time (Johnson et al., 2020).

We developed the following scoring system to track the worsening of eye phenotypes for this study: score 1) normal (wild-type-looking) eye; score 2) loss of the pseudopupil; score 3) early signs of color variegation throughout the eye in addition to pseudopupil loss; score 4) depigmentation of a portion of the eye in addition to color variegation and pseudopupil loss (Fig. 5A). Eyes were scored weekly for six weeks following eclosion using the scale described above, with a higher score indicating a worse phenotype. As shown in Fig. 5B and C, the presence of N-VCP significantly improved eye phenotypes beginning at day 14 and continuing for the remainder of the study. Fig. 5B shows the average score for each group at each time point, while Fig. 5C expands those averages to display the proportion of each score in each group at a given time point to provide further visualization of the worsening phenotype over time. Thus, just as with other tissues, N-VCP suppresses toxicity from pathogenic ataxin-3 in fly eyes.

A strong molecular indicator of toxicity and disease progression in polyQ disease models is the level of disease protein aggregation (Costa and Paulson, 2012; Klockgether et al., 2019; Lieberman et al., 2019; Paulson et al., 1997; Todi et al., 2007a). In our studies using *Drosophila* SCA models, we found that aggregation of pathogenic ataxin-3 and other polyQ proteins precedes toxicity (Johnson et al., 2019; Johnson et al., 2020; Ristic et al., 2018; Sutton et al., 2017; Tsou et al., 2013; Tsou et al., 2015a; Tsou et al., 2015b; Tsou et al., 2016). We also observed that the level of aggregation of these proteins correlates with the extent of their pathogenicity (Johnson et al., 2019; Johnson et al., 2020; Ristic et al., 2018; Sutton et al., 2017; Tsou et al., 2013; Tsou et al., 2015a; Tsou et al., 2015b; Tsou et al., 2016). Next, we sought to examine this relationship in fly eyes.

Author Manuscript Author Manuscript Author Manuscript Author Manuscript

To assess ataxin-3 aggregation, we performed Western blot analyses using lysates from dissected fly heads expressing the 'stronger' pathogenic ataxin-3 alone or alongside Myc-tagged N-VCP (Fig. 6A). The presence of N-VCP seemed to increase the amount of SDS-soluble ataxin-3 (Fig. 6A, green outlines). Lanes with lysates from flies expressing pathogenic ataxin-3 alone have lower amounts of SDS-soluble ataxin-3 in comparison to those also expressing N-VCP (Fig. 6A, green outlines); additionally, the level of SDS-resistant ataxin-3 appears higher in the absence of N-VCP (Fig. 6A, orange outlines), indicative of increased levels of aggregated species that migrate more slowly through SDS-PAGE gels. Since these blots suggested that the presence of N-VCP reduces aggregated species of pathogenic ataxin-3, we sought to confirm these results through the utilization of filter-trap assays. These assays take advantage of a porous nitrocellulose membrane that, when a sample is passed through it via suction, captures higher-order aggregated protein species (Chang and Kuret, 2008; Johnson et al., 2019; Johnson et al., 2020; Weishäupl et al., 2019; Xu et al., 2002). Lysates from flies expressing pathogenic ataxin-3 alone or with N-VCP showed that the presence of the truncated protein significantly reduced the amount of aggregated ataxin-3 trapped on the membrane (Fig. 6B). From these data we conclude that N-VCP leads to reduced levels of aggregated, pathogenic ataxin-3.

### 3.5. Dose-dependent effects of N-VCP

Thus far, we observed improvement in developmental progression, longevity, eye phenotypes, and pathogenic ataxin-3 aggregation of SCA3 models because of co-expression of the N-terminal VCP truncated protein (Figs. 2–6). We also observed a significant worsening of developmental outcomes with overexpression of full-length VCP in those same SCA3 models (Supplemental Fig. 4). As we already confirmed improvement from a single copy of N-VCP, and an increased copy number of full-length VCP intensified SCA3 toxicity (Supplemental Fig. 4), we next asked the question: can an additional copy of N-VCP further ameliorate SCA3 toxicity in flies?

We returned to the fly eye as our model with *Drosophilae* containing either zero, one, or two copies of the N-VCP transgene alongside the 'stronger' pathogenic ataxin-3. Just as in Fig. 5, eyes were scored on a weekly basis for six weeks following eclosion; however, the scoring scale for this set of studies was expanded to account for what we thought might be more subtle differences among flies expressing one versus two copies of N-VCP. This new scale is as follows: score 1) normal (wild-type-looking) eye with a clear pseudopupil; score 2) weaker pseudopupil that has begun to fade and lose its clear shape; score 3) undetectable pseudopupil; score 4) color variegation at the edge of the eye in addition to pseudopupil loss; score 5) widerspread depigmentation throughout the eye in addition to color variegation and pseudopupil loss (Fig. 7A). Multiple statistical comparisons were made among the groups to detect differences among the varying copy numbers of the N-VCP transgene.

Beginning on day 7, we observed significant improvement in eye phenotype in the presence of both one (validating the observations of Fig. 5) and two copies of N-VCP compared to expression of the 'stronger' pathogenic ataxin-3 alone (Fig. 7B). Additionally, starting on day 14, the data revealed a significant improvement comparing one copy to two copies of N-VCP (Fig. 7B). Just as in Fig. 5, 7B shows the average score for each group at each

Author Manuscript Author Manuscript Author Manuscript Author Manuscript

time point, while Fig. 7C expands those averages to display the proportion of each score in each group at a given time point. The differences among the three groups persisted for the remainder of the observation timeline with a single copy of N-VCP improving eye phenotypes over ataxin-3 alone, and two copies of N-VCP showing improvement over both of the other groups. This indicates that the response from N-VCP on ataxin-3-dependent phenotypes is dose-dependent.

### 3.6. N-VCP reduces pathogenic ataxin-3 aggregation in a dose-dependent manner

As with a single copy of the N-VCP transgene, we again assessed whether phenotypic improvement observed with two copies of N-VCP coincides with further reduction in ataxin-3 aggregation. Analyses of Western blots from dissected fly heads from each line showed that there is a significant increase in the amount of N-VCP from one copy of the transgene to two, and that this increase in N-VCP does not result in significant reduction of total ataxin-3 protein levels (Fig. 8A).

We then focused on SDS-soluble and -resistant ataxin-3. As outlined in Fig. 8A, the amount of SDS-soluble ataxin-3 appears to increase in the presence of N-VCP (Fig. 8A, green outlines) coincident with a decrease in SDS-resistant species (Fig. 8A, orange outlines). This apparent decrease in aggregated ataxin-3 was validated with filter-trap assays, which revealed a steady decrease in higher-order ataxin-3 species from zero to one and zero to two copies of the N-VCP transgene (Fig. 8B). There was also a trend in reduced levels of filter-trapped pathogenic ataxin-3 when comparing one vs. two copies of N-VCP (Fig. 8B). This trend did not reach statistical significance with ANOVA ($p = 0.086$) when comparing one copy vs. two copies, but did reach significance with a student's *t*-test ($p = 0.012$), overall supporting the notion that higher levels of N-VCP lead to increased reduction of higher-order ataxin-3 species.

Lastly, we examined whether N-VCP impacts ataxin-3 binding to endogenous VCP. Through co-IPs for HA-tagged ataxin-3 using dissected fly heads, we observed that N-VCP significantly reduced the amount of endogenous VCP that co-IPed with pathogenic ataxin-3 compared to ataxin-3 alone (Fig. 8C). We conclude that N-VCP reduces the interaction of ataxin-3 with endogenous VCP and leads to lower levels of aggregated, pathogenic ataxin-3.

## 4. Discussion

Domains outside of the polyQ repeat play important roles in the pathogenicity of polyQ disease proteins. For the SCA3 protein, ataxin-3, we and others reported that the polyQ-adjacent VBM is important for its interaction with the hexameric protein, VCP (Boeddrich et al., 2006; Ristic et al., 2018; Wang et al., 2006; Wang et al., 2008; Zhong and Pittman, 2006). We also found that VCP exacerbates the toxicity of human, full-length, pathogenic ataxin-3 in fly models of SCA3 (Ristic et al., 2018). Based on those data (Ristic et al., 2018); on studies by others that investigated the interaction of ataxin-3 with VCP (Boeddrich et al., 2006); and on studies that investigated ataxin-3 aggregation in vitro — a two-step process where the N-termini of ataxin-3 proteins interact and facilitate subsequent polyQ length-dependent fibrilization (Ellisdon et al., 2006; Masino et al., 2011; Masino et al., 2004; Ristic et al., 2018) — a model emerged where VCP hexamers binding to multiple

Author Manuscript Author Manuscript Author Manuscript Author Manuscript

pathogenic ataxin-3 proteins raise their local concentration and likelihood of interacting and aggregating (Fig. 9, top). This model was supported by our prior data that preventing the binding of pathogenic ataxin-3 to VCP through genetic mutations, or knocking down endogenous VCP, decreases pathogenic ataxin-3 aggregation and toxicity in *Drosophila* (Ristic et al., 2018). The VBM of ataxin-3 was reported to contain a nuclear-localization signal (Albrecht et al., 2004); however, based on our earlier research, the VBM does not impact ataxin-3's subcellular localization in *Drosophila* (Ristic et al., 2018). Thus, it is unlikely that interventions involving the VBM impact the sub-cellular localization of pathogenic ataxin-3. Collectively, these studies identified the VBM of pathogenic ataxin-3 as a potential targeting site to combat SCA3.

Here, we presented evidence that engaging the VBM of pathogenic ataxin-3 with a truncated protein — the N-terminus of VCP lacking the domains necessary to homo-hexamerise — ameliorates ataxin-3-dependent toxicity in flies. Phenotypic improvement coincided with reduced aggregation of pathogenic ataxin-3 and diminished binding of the SCA3 protein to VCP. Our observations from this work further inform the working model in Fig. 9. We propose that VCP-dependent aggregation of pathogenic ataxin-3 can be decelerated through the introduction of the N-VCP truncated protein that displaces the VCP-ataxin-3 interaction (Fig. 9, bottom). These results strengthen the rationale to pursue the VBM of ataxin-3 as a potential target for SCA3 intervention.

Ataxin-3 and VCP have been proposed to cooperate functionally in endoplasmic reticulum-associated protein degradation (ERAD) (Morreale et al., 2009; Wang et al., 2006; Wang et al., 2008; Zhong and Pittman, 2006). The retro-translocation to the cytosol of substrates produced in the ER lumen is a critical step in this branch of proteasome-associated protein quality control. Ataxin-3's DUB activity has been implicated in regulating the flow of ERAD substrates in a VCP binding-dependent manner (Morreale et al., 2009; Wang et al., 2006; Wang et al., 2008; Zhong and Pittman, 2006). Other protein partners of VCP possess a similar VBM and may compete with ataxin-3 to bind VCP, further regulating the retro-translocation process (Morreale et al., 2009). Prior studies suggested that one of ataxin-3's normal functions is to modulate ERAD by altering VCP's ability to facilitate protein retro-translocation (Morreale et al., 2009; Wang et al., 2006; Wang et al., 2008; Zhong and Pittman, 2006). However, the physiological significance of the ataxin-3-VCP interaction in vivo is not entirely clear, since *Atxn3* knockout mice appear normal (Schmitt et al., 2007; Switonski et al., 2011; Zeng et al., 2013), suggesting either that ataxin-3 is not fully, or always, required for ERAD-dependent processes, or that another DUB is able to conduct its functions when it is absent. Further uncovering the functional nature of ataxin-3's interaction with VCP, and whether that interaction is a part of a unique action, is important in understanding ataxin-3's physiological roles.

The RXXR sequence (where 'X' denotes any amino acid) within a predicted $\alpha$-helix that comprises the VBM is not exclusive to ataxin-3. The ubiquitin ligase E4b (Ube4b), ubiquitin fusion degradation protein 2a (Ufd2a), hydroxymethylglutaryl reductase degradation protein (Hrd1) (also known as Synoviolin 1), and the ER-resident ubiquitin ligase $M_r$ 78,000 glycoprotein (gp78) all possess a version of this sequence that can bind directly to the N-terminus of VCP (Morreale et al., 2009); *Drosophila* has well conserved orthologues

Author Manuscript Author Manuscript Author Manuscript Author Manuscript

of these genes and their peptides also contain the RXXR sequence (Larkin et al., 2021). Each of these proteins is involved in ERAD (Morreale et al., 2009). Their function can be influenced by the mutual exclusivity of their interaction with VCP in direct competition with other VCP-interacting proteins (Morreale et al., 2009). While these VBM-containing proteins may be involved in similar pathways, their distinct interactions, competitions, and variability in cofactor binding allows each of them to have unique roles in ERAD (Morreale et al., 2009). Because of these interactions, one might have considered that the N-VCP approach we described here could have led to deleterious effects. While N-VCP consistently suppressed toxicity from pathogenic ataxin-3, it enhanced the toxicity of pathogenic ataxin-3 with mutated VBM and of the SCA6 protein (Fig. 4). These observations suggest the possibility that N-VCP disrupts some cellular processes during misfolded protein stress, perhaps by interacting with other VBM-containing proteins; the truncated protein, however, does not appear to be detrimental under normal conditions in the fly (Fig. 1 and Supplemental Fig. 1). The future aim of this investigation is to inhibit direct binding of ataxin-3 to VCP through a highly targeted, small molecule design; that approach would presumably circumvent the above possibility.

The ultimate goal for studying SCA3 is to devise therapeutic interventions for it. As the SCA3 therapeutics field forges ahead, interventions focused on biomarkers; mechanistic targets that may upregulate specific pathways, such as autophagy; oligonucleotide-based targeting of the *ATXN3* mRNA; and others are being considered to mitigate ataxin-3-based toxicity (Chen et al., 2020; Costa et al., 2016; Da Silva et al., 2019; Johnson et al., 2019; Johnson et al., 2020; Matos et al., 2019; Moore et al., 2019; Scaglione et al., 2011; Sutton et al., 2017; Tsou et al., 2015b). To this list we add the ataxin-3-VCP interaction and the VBM as another potential therapeutic entry point. N-VCP is too large to be a deliverable; however, the basic concept that we presented here can be utilized to design or discover compounds that disrupt the interaction of ataxin-3 with VCP. Since there is benefit from the approach we described here, studies that further evaluate this disruption at a structural level and weaponize it against SCA3 will likely prove beneficial.

To conclude, targeting the VBM of pathogenic ataxin-3 brings phenotypic benefits in fly models of SCA3 and provides further evidence of the importance of protein-protein interactions in the etiology of SCA3 and of other, similar diseases.

## Supplementary Material

Refer to Web version on PubMed Central for supplementary material.

## Funding information

This work was supported in part by a Competitive Graduate Research Assistantship to SLJ by Wayne State University Graduate School, by a Thomas Rumble Fellowship to SLJ by Wayne State University Graduate School, by a Thomas Rumble Fellowship to JRB by Wayne State University Graduate School, and by R01NS08677 to SVT from NINDS.

Author Manuscript Author Manuscript Author Manuscript Author Manuscript

## References


Albrecht M, et al. , 2004. Structural and functional analysis of ataxin-2 and ataxin-3. Eur. J. Biochem. 271, 3155–3170. [PubMed: 15265035]

Ashraf NS, et al. , 2020. Druggable genome screen identifies new regulators of the abundance and toxicity of ATXN3, the spinocerebellar Ataxia type 3 disease protein. Neurobiol. Dis. 137, 104697. [PubMed: 31783119]

Berke SJ, et al. , 2005. Defining the role of ubiquitin-interacting motifs in the polyglutamine disease protein, ataxin-3. J. Biol. Chem. 280, 32026–32034. [PubMed: 16040601]

Blount JR, et al. , 2012. Ubiquitin-specific protease 25 functions in endoplasmic reticulum-associated degradation. PLoS One 7, e36542. [PubMed: 22590560]

Blount JR, et al. , 2014. Ubiquitin-binding site 2 of ataxin-3 prevents its proteasomal degradation by interacting with Rad23. Nat. Commun. 5, 4638. [PubMed: 25144244]

Blount JR, et al. , 2018. Expression and regulation of Deubiquitinase-resistant, unanchored ubiquitin chains in Drosophila. Sci. Rep 8, 8513. [PubMed: 29855490]

Blount JR, et al. , 2020. Isoleucine 44 hydrophobic patch controls toxicity of unanchored, linear ubiquitin chains through NF-κB signaling. Cells 9.

Boeddrich A, et al. , 2006. An arginine/lysine-rich motif is crucial for VCP/p97-mediated modulation of ataxin-3 fibrillogenesis. EMBO J. 25, 1547–1558. [PubMed: 16525503]

Buchberger A, et al. , 2010. Protein quality control in the cytosol and the endoplasmic reticulum: brothers in arms. Mol. Cell 40, 238–252. [PubMed: 20965419]

Burr AA, et al. , 2014. Using membrane-targeted green fluorescent protein to monitor neurotoxic protein-dependent degeneration of Drosophila eyes. J. Neurosci. Res. 92, 1100–1109. [PubMed: 24798551]

Cancel G, et al. , 1995. Marked phenotypic heterogeneity associated with expansion of a CAG repeat sequence at the spinocerebellar ataxia 3/Machado-Joseph disease locus. Am. J. Hum. Genet. 57, 809–816. [PubMed: 7573040]

Chang E, Kuret J, 2008. Detection and quantification of tau aggregation using a membrane filter assay. Anal. Biochem. 373, 330–336. [PubMed: 17949677]

Chen YS, et al. , 2020. Identifying therapeutic targets for spinocerebellar Ataxia type 3/ Machado-Joseph disease through integration of pathological biomarkers and therapeutic strategies. Int. J. Mol. Sci 21.

Costa MDC, et al. , 2016. Unbiased screen identifies aripiprazole as a modulator of abundance of the polyglutamine disease protein, ataxin-3. Brain. 139, 2891–2908. [PubMed: 27645800]

Costa MOC, Paulson HL, 2012. Toward understanding Machado-Joseph disease. Prog. Neurobiol. 97, 239–257. [PubMed: 22133674]

Coutinho P, Andrade C, 1978. Autosomal dominant system degeneration in Portuguese families of the Azores Islands. A new genetic disorder involving cerebellar, pyramidal, extrapyramidal and spinal cord motor functions. Neurology. 28, 703–709. [PubMed: 566869]

Da Silva JD, et al. , 2019. From pathogenesis to novel therapeutics for spinocerebellar Ataxia type 3: evading potholes on the way to translation. Neurotherapeutics. 16, 1009–1031. [PubMed: 31691128]

Dai RM, et al. , 1998. Involvement of valosin-containing protein, an ATPase co-purified with IkappaBalpha and 26 S proteasome, in ubiquitin-proteasome-mediated degradation of IkappaBalpha. J. Biol. Chem. 273, 3562–3573. [PubMed: 9452483]

Dantuma NP, Herzog LK, 2020. Machado-Joseph disease: a stress combating deubiquitylating enzyme changing sides. Adv. Exp. Med. Biol. 1233, 237–260. [PubMed: 32274760]

DeLaBarre B, et al. , 2006. Central pore residues mediate the p97/VCP activity required for ERAD. Mol. Cell 22, 451–462. [PubMed: 16713576]

Du X, et al. , 2013. Second cistron in CACNA1A gene encodes a transcription factor mediating cerebellar development and SCA6. Cell. 154, 118–133. [PubMed: 23827678]

Dürr A, et al. , 1996. Spinocerebellar ataxia 3 and Machado-Joseph disease: clinical, molecular, and neuropathological features. Ann. Neurol. 39, 490–499. [PubMed: 8619527]

Author Manuscript Author Manuscript Author Manuscript Author Manuscript

Ellisdon AM, et al. , 2006. The two-stage pathway of ataxin-3 fibrillogenesis involves a polyglutamine-independent step. J. Biol. Chem. 281, 16888–16896. [PubMed: 16624810]

Fish MP, et al. , 2007. Creating transgenic Drosophila by microinjecting the site-specific phiC31 integrase mRNA and a transgene-containing donor plasmid. Nat. Protoc. 2, 2325–2331. [PubMed: 17947973]

Franceschini A, et al. , 2016. SVD-phy: improved prediction of protein functional associations through singular value decomposition of phylogenetic profiles. Bioinformatics. 32, 1085–1087. [PubMed: 26614125]

Friedman JH, 2002. Presumed rapid eye movement behavior disorder in Machado-Joseph disease (spinocerebellar ataxia type 3). Mov. Disord. 17, 1350–1353. [PubMed: 12465081]

Friedman JH, et al. , 2003. REM behavior disorder and excessive daytime somnolence in Machado-Joseph disease (SCA-3). Mov. Disord. 18, 1520–1522. [PubMed: 14673890]

Fujita K, et al. , 2013. A functional deficiency of TERA/VCP/p97 contributes to impaired DNA repair in multiple polyglutamine diseases. Nat. Commun. 4, 1816. [PubMed: 23652004]

Groth AC, et al. , 2004. Construction of transgenic Drosophila by using the site-specific integrase from phage phiC31. Genetics. 166, 1775–1782. [PubMed: 15126397]

Harris GM, et al. , 2010. Splice isoforms of the polyglutamine disease protein ataxin-3 exhibit similar enzymatic yet different aggregation properties. PLoS One 5, e13695. [PubMed: 21060878]

Johnson SL, et al. , 2019. Differential toxicity of ataxin-3 isoforms in Drosophila models of spinocerebellar Ataxia type 3. Neurobiol. Dis. 132, 104535. [PubMed: 31310802]

Johnson SL, et al. , 2020. Ubiquitin-interacting motifs of ataxin-3 regulate its polyglutamine toxicity through Hsc70–4-dependent aggregation. Elife 9.

Kawaguchi Y, et al. , 1994. CAG expansions in a novel gene for Machado-Joseph disease at chromosome 14q32.1. Nat. Genet. 8, 221–228. [PubMed: 7874163]

Kim NC, et al. , 2013. VCP is essential for mitochondrial quality control by PINK1/ Parkin and this function is impaired by VCP mutations. Neuron. 78, 65–80. [PubMed: 23498974]

Klockgether T, et al. , 2019. Spinocerebellar ataxia. Nat Rev Dis Primers. 5, 24. [PubMed: 30975995]

Kobayashi T, et al. , 2002. Functional ATPase activity of p97/valosin-containing protein (VCP) is required for the quality control of endoplasmic reticulum in neuronally differentiated mammalian PC12 cells. J. Biol. Chem. 277, 47358–47365. [PubMed: 12351637]

Larkin A, et al. , 2021. FlyBase: updates to the *Drosophila melanogaster* knowledge base. Nucleic Acids Res. 49, D899–D907. [PubMed: 33219682]

Li X, et al. , 2015. Toward therapeutic targets for SCA3: insight into the role of Machado-Joseph disease protein ataxin-3 in misfolded proteins clearance. Prog. Neurobiol. 132, 34–58. [PubMed: 26123252]

Lieberman AP, et al. , 2019. Polyglutamine repeats in neurodegenerative diseases. Annu. Rev. Pathol. 14, 1–27. [PubMed: 30089230]

Lin KP, Soong BW, 2002. Peripheral neuropathy of Machado-Joseph disease in Taiwan: a morphometric and genetic study. Eur. Neurol. 48, 210–217. [PubMed: 12422070]

Masino L, et al. , 2004. Characterization of the structure and the amyloidogenic properties of the Josephin domain of the polyglutamine-containing protein ataxin-3. J. Mol. Biol. 344, 1021–1035. [PubMed: 15544810]

Masino L, et al. , 2011. The Josephin domain determines the morphological and mechanical properties of ataxin-3 fibrils. Biophys. J. 100, 2033–2042. [PubMed: 21504740]

Matos CA, et al. , 2011. Polyglutamine diseases: the special case of ataxin-3 and Machado-Joseph disease. Prog. Neurobiol. 95, 26–48. [PubMed: 21740957]

Matos CA, et al. , 2019. Machado-Joseph disease/spinocerebellar ataxia type 3: lessons from disease pathogenesis and clues into therapy. J. Neurochem. 148, 8–28. [PubMed: 29959858]

Matsumura R, et al. , 1996. The relationship between trinucleotide repeat length and phenotypic variation in Machado-Joseph disease. J. Neurol. Sci. 139, 52–57. [PubMed: 8836972]

Meyer H, et al. , 2012. Emerging functions of the VCP/p97 AAA-ATPase in the ubiquitin system. Nat. Cell Biol. 14, 117–123. [PubMed: 22298039]

Author Manuscript Author Manuscript Author Manuscript Author Manuscript

Moore LR, et al. , 2019. Antisense oligonucleotide therapy rescues aggresome formation in a novel spinocerebellar ataxia type 3 human embryonic stem cell line. Stem Cell Res. 39, 101504. [PubMed: 31374463]

Mori-Konya C, et al. , 2009. p97/valosin-containing protein (VCP) is highly modulated by phosphorylation and acetylation. Genes Cells 14, 483–497. [PubMed: 19335618]

Morreale G, et al. , 2009. Evolutionary divergence of valosin-containing protein/cell division cycle protein 48 binding interactions among endoplasmic reticulum-associated degradation proteins. FEBS J 276, 1208–1220. [PubMed: 19175675]

Nath SR, Lieberman AP, 2017. The ubiquitination, disaggregation and proteasomal degradation machineries in Polyglutamine disease. Front. Mol. Neurosci. 10, 78. [PubMed: 28381987]

Nicastro G, et al. , 2009. Josephin domain of ataxin-3 contains two distinct ubiquitin-binding sites. Biopolymers. 91, 1203–1214. [PubMed: 19382171]

Nicastro G, et al. , 2010. Understanding the role of the Josephin domain in the PolyUb binding and cleavage properties of ataxin-3. PLoS One 5, e12430. [PubMed: 20865150]

Pandey M, Rajamma U, 2018. Huntington's disease: the coming of age. J. Genet. 97, 649–664. [PubMed: 30027901]

Paulson H, 2012. Machado-Joseph disease/spinocerebellar ataxia type 3. Handb. Clin. Neurol. 103, 437–449. [PubMed: 21827905]

Paulson HL, et al. , 1997. Machado-Joseph disease gene product is a cytoplasmic protein widely expressed in brain. Ann. Neurol. 41, 453–462. [PubMed: 9124802]

Paulson HL, et al. , 2017. Polyglutamine spinocerebellar ataxias - from genes to potential treatments. Nat. Rev. Neurosci. 18, 613–626. [PubMed: 28855740]

Pérez Ortiz JM, Orr HT, 2018. Spinocerebellar Ataxia type 1: molecular mechanisms of neurodegeneration and preclinical studies. Adv. Exp. Med. Biol. 1049, 135–145. [PubMed: 29427101]

Ranum LP, et al. , 1995. Spinocerebellar ataxia type 1 and Machado-Joseph disease: incidence of CAG expansions among adult-onset ataxia patients from 311 families with dominant, recessive, or sporadic ataxia. Am. J. Hum. Genet. 57, 603–608. [PubMed: 7668288]

Ristic G, et al. , 2018. Toxicity and aggregation of the polyglutamine disease protein, ataxin-3 is regulated by its binding to VCP/p97 in *Drosophila melanogaster*. Neurobiol. Dis. 116, 78–92. [PubMed: 29704548]

Rosenberg RN, 1992. Machado-Joseph disease: an autosomal dominant motor system degeneration. Mov. Disord. 7, 193–203. [PubMed: 1620135]

Rüb U, et al. , 2002a. Degeneration of the external cuneate nucleus in spinocerebellar ataxia type 3 (Machado-Joseph disease). Brain Res. 953, 126–134. [PubMed: 12384246]

Rüb U, et al. , 2002b. Spinocerebellar ataxia type 3 (Machado-Joseph disease): severe destruction of the lateral reticular nucleus. Brain. 125, 2115–2124. [PubMed: 12183356]

Rüb U, et al. , 2003. The nucleus raphe interpositus in spinocerebellar ataxia type 3 (Machado-Joseph disease). J. Chem. Neuroanat. 25, 115–127. [PubMed: 12663059]

Rüb U, et al. , 2004a. Degeneration of the central vestibular system in spinocerebellar ataxia type 3 (SCA3) patients and its possible clinical significance. Neuropathol. Appl. Neurobiol. 30, 402–414. [PubMed: 15305986]

Rüb U, et al. , 2004b. Damage to the reticulotegmental nucleus of the pons in spinocerebellar ataxia type 1, 2, and 3. Neurology. 63, 1258–1263. [PubMed: 15477548]

Sasaki H, et al. , 1995. CAG repeat expansion of Machado-Joseph disease in the Japanese: analysis of the repeat instability for parental transmission, and correlation with disease phenotype. J. Neurol. Sci. 133, 128–133. [PubMed: 8583215]

Scaglione KM, et al. , 2011. Ube2w and ataxin-3 coordinately regulate the ubiquitin ligase CHIP. Mol. Cell 43, 599–612. [PubMed: 21855799]

Schmitt I, et al. , 2007. Inactivation of the mouse Atxn3 (ataxin-3) gene increases protein ubiquitination. Biochem. Biophys. Res. Commun. 362, 734–739. [PubMed: 17764659]

Author Manuscript Author Manuscript Author Manuscript Author Manuscript

Schöls L, et al. , 1996. Relations between genotype and phenotype in German patients with the Machado-Joseph disease mutation. J. Neurol. Neurosurg. Psychiatry 61, 466–470. [PubMed: 8937340]

Schöls L, et al. , 2004. Therapeutic strategies in Friedreich's ataxia. J. Neural Transm. Suppl 135–145. [PubMed: 15354399]

Sequeiros J, Coutinho P, 1993. Epidemiology and clinical aspects of Machado-Joseph disease. Adv. Neurol. 61, 139–153. [PubMed: 8421964]

Soong B, et al. , 1997. Machado-Joseph disease: clinical, molecular, and metabolic characterization in Chinese kindreds. Ann. Neurol. 41, 446–452. [PubMed: 9124801]

Sujkowski A, et al. , 2015. Endurance exercise and selective breeding for longevity extend Drosophila healthspan by overlapping mechanisms. Aging (Albany NY) 7, 535–552. [PubMed: 26298685]

Sutton JR, et al. , 2017. Interaction of the polyglutamine protein ataxin-3 with Rad23 regulates toxicity in Drosophila models of spinocerebellar Ataxia type 3. Hum. Mol. Genet. 26, 1419–1431. [PubMed: 28158474]

Switonski PM, et al. , 2011. Mouse ataxin-3 functional knock-out model. NeuroMolecular Med. 13, 54–65. [PubMed: 20945165]

Szklarczyk D, et al. , 2017. The STRING database in 2017: quality-controlled protein-protein association networks, made broadly accessible. Nucleic Acids Res. 45, D362–D368. [PubMed: 27924014]

Szklarczyk D, et al. , 2019. STRING v11: protein-protein association networks with increased coverage, supporting functional discovery in genome-wide experimental datasets. Nucleic Acids Res. 47, D607–D613. [PubMed: 30476243]

Takiyama Y, et al. , 1993. The gene for Machado-Joseph disease maps to human chromosome 14q. Nat. Genet. 4, 300–304. [PubMed: 8358439]

Takiyama Y, et al. , 1994. A clinical and pathologic study of a large Japanese family with Machado-Joseph disease tightly linked to the DNA markers on chromosome 14q. Neurology. 44, 1302–1308. [PubMed: 8035935]

Todi SV, et al., 2007a. Polyglutamine disorders including huntington's disease. In: G WS (Ed.), Molecular Neurology. Academic Press, pp. 257–276.

Todi SV, et al. , 2007b. Cellular turnover of the polyglutamine disease protein ataxin-3 is regulated by its catalytic activity. J. Biol. Chem. 282, 29348–29358. [PubMed: 17693639]

Todi SV, et al. , 2009. Ubiquitination directly enhances activity of the deubiquitinating enzyme ataxin-3. EMBO J. 28, 372–382. [PubMed: 19153604]

Tsou WL, et al. , 2013. Ubiquitination regulates the neuroprotective function of the deubiquitinase ataxin-3 in vivo. J. Biol. Chem. 288, 34460–34469. [PubMed: 24106274]

Tsou WL, et al. , 2015a. DnaJ-1 and karyopherin α3 suppress degeneration in a new Drosophila model of spinocerebellar Ataxia type 6. Hum. Mol. Genet. 24, 4385–4396. [PubMed: 25954029]

Tsou WL, et al. , 2015b. The deubiquitinase ataxin-3 requires Rad23 and DnaJ-1 for its neuroprotective role in *Drosophila melanogaster*. Neurobiol. Dis. 82, 12–21. [PubMed: 26007638]

Tsou WL, et al. , 2016. Polyglutamine length-dependent toxicity from a1ACT in Drosophila models of spinocerebellar ataxia type 6. Biol Open. 5, 1770–1775. [PubMed: 27979829]

Wang Q, et al. , 2003. Hexamerization of p97-VCP is promoted by ATP binding to the D1 domain and required for ATPase and biological activities. Biochem. Biophys. Res. Commun. 300, 253–260. [PubMed: 12504076]

Wang Q, et al. , 2006. Regulation of retrotranslocation by p97-associated deubiquitinating enzyme ataxin-3. J. Cell Biol. 174, 963–971. [PubMed: 17000876]

Wang Q, et al. , 2008. Inhibition of p97-dependent protein degradation by Eeyarestatin I. J. Biol. Chem. 283, 7445–7454. [PubMed: 18199748]

Watanabe H, et al. , 1998. Frequency analysis of autosomal dominant cerebellar ataxias in Japanese patients and clinical characterization of spinocerebellar ataxia type 6. Clin. Genet. 53, 13–19. [PubMed: 9550356]

Weishäupl D, et al. , 2019. Physiological and pathophysiological characteristics of ataxin-3 isoforms. J. Biol. Chem. 294, 644–661. [PubMed: 30455355]

Author Manuscript Author Manuscript Author Manuscript Author Manuscript

Winborn BJ, et al. , 2008. The deubiquitinating enzyme ataxin-3, a polyglutamine disease protein, edits Lys63 linkages in mixed linkage ubiquitin chains. J. Biol. Chem. 283, 26436–26443. [PubMed: 18599482]

Xu G, et al. , 2002. Rapid detection of protein aggregates in the brains of Alzheimer patients and transgenic mouse models of amyloidosis. Alzheimer Dis. Assoc. Disord. 16, 191–195. [PubMed: 12218651]

Zeng L, et al. , 2013. The de-ubiquitinating enzyme ataxin-3 does not modulate disease progression in a knock-in mouse model of Huntington disease. J Huntingtons Dis 2, 201–215. [PubMed: 24683430]

Zhong X, Pittman RN, 2006. Ataxin-3 binds VCP/p97 and regulates retrotranslocation of ERAD substrates. Hum. Mol. Genet. 15, 2409–2420. [PubMed: 16822850]

Zhou YX, et al. , 1997. Machado-Joseph disease in four Chinese pedigrees: molecular analysis of 15 patients including two juvenile cases and clinical correlations. Neurology. 48, 482–485. [PubMed: 9040742]

Zoghbi HY, Orr HT, 2009. Pathogenic mechanisms of a polyglutamine-mediated neurodegenerative disease, spinocerebellar ataxia type 1. J. Biol. Chem. 284, 7425–7429. [PubMed: 18957430]

Author Manuscript Author Manuscript Author Manuscript Author Manuscript

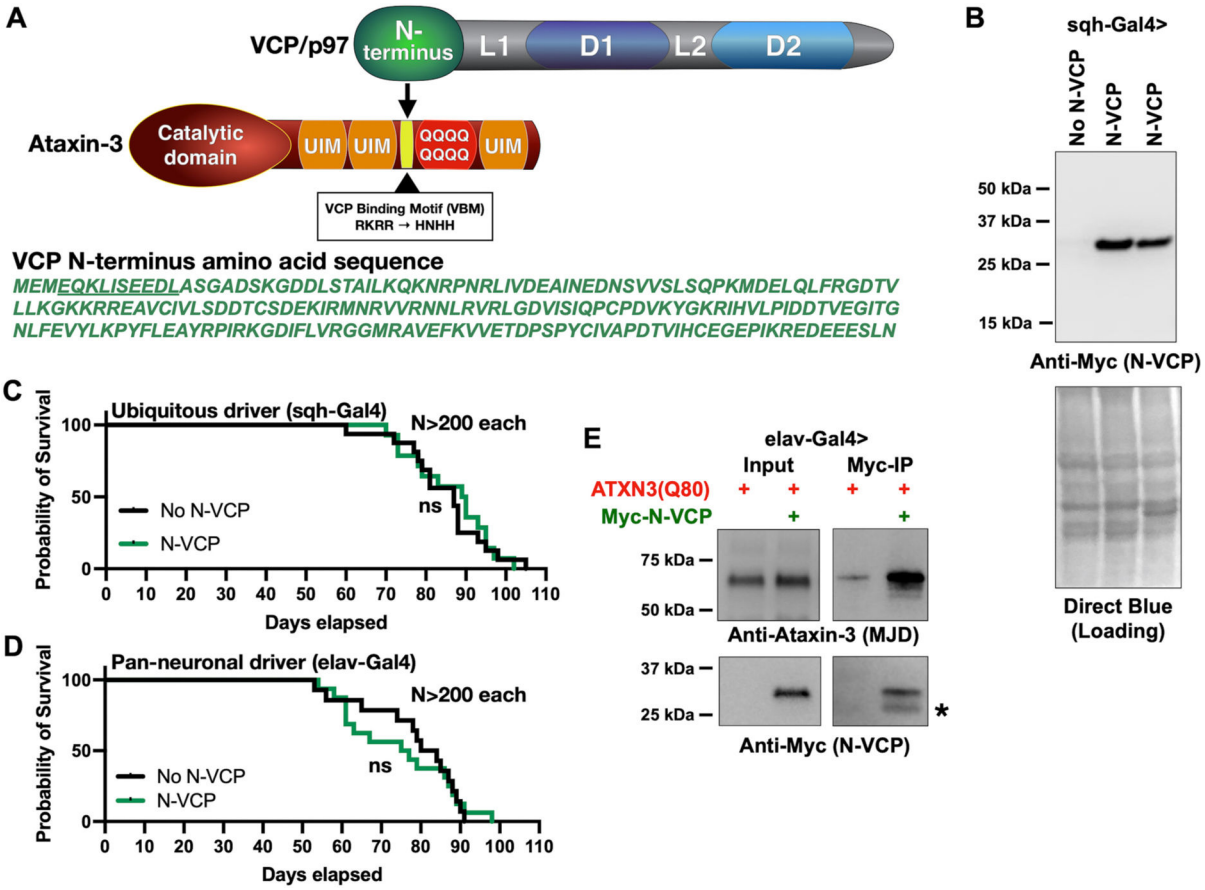


**Fig. 1.**

N-VCP is non-toxic in *Drosophila* and interacts with pathogenic ataxin-3.

(A) Diagrammatic representation of the VCP-ataxin-3 interaction and the amino acid sequence of N-VCP. For VCP: L1/L2, linker domains; D1/D2, D1 and D2 domains. For ataxin-3: UIM, ubiquitin-interacting motif; "QQQ", polyQ region that causes SCA3 when expanded abnormally. (B) Western blot from lysates of whole flies expressing N-VCP ubiquitously. Lysates from two independent experiments are shown. (C) Survival analyses of flies expressing N-VCP ubiquitously (sqh-Gal4). Control: flies that contain the ubiquitous driver without N-VCP. "ns": non-statistically significant; log-rank test. (D) Survival analyses of flies expressing N-VCP pan-neuronally (elav-Gal4). Control: flies that contain the pan-neuronal driver without N-VCP. "ns": non-statistically significant; log-rank test. (E) Co-immunopurification performed with anti-Myc antibody-tagged beads to precipitate Myc-N-VCP. Pan-neuronal driver: elav-Gal4. Asterisk: band that we observe sometimes with Myc-N-VCP and that may represent a proteolytic species.

Author Manuscript Author Manuscript Author Manuscript Author Manuscript

A

| Fly Line | Description | Expression | Outcome |
|---|---|---|---|
| No pathogenic ATXN3 | Genetic background used to generate transgenic flies | Not applicable | Normal development and adult fly longevity |
| ATXN3-Weaker (Q77) | Pathogenic ataxin-3 inserted at chromosomal site attP2. Expresses at lower protein levels than "stronger" line | Ubiquitous | Marked developmental death; a handful of adult flies eclosed and were all dead by 40 days; figure 2 |
| ATXN3-Stronger (Q80) | Pathogenic ataxin-3 inserted at chromosomal site attP2; optimized Kozak sequence. Expresses at higher protein levels than "weaker" line | Ubiquitous | Marked developmental lethality. No adult flies eclosed; figure 3 |

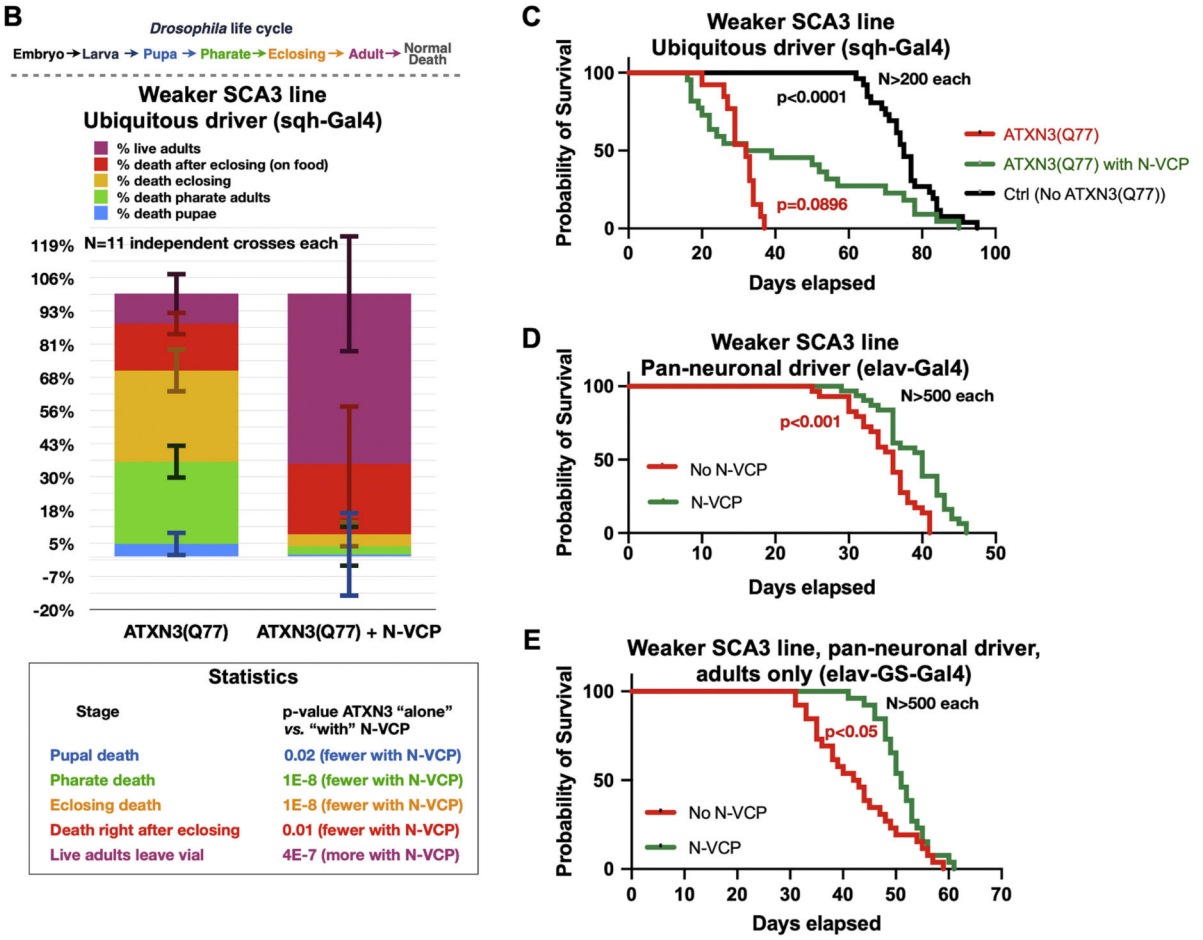


**Fig. 2.**

N-VCP reduces toxicity from pathogenic ataxin-3 with 77Q.

(A) Summary of the pathogenic ataxin-3 and control fly lines along with outcomes of their ubiquitous expression in the absence of N-VCP. Driver: sqh-Gal4. (B) Observations of developmental lethality in flies ubiquitously expressing 'weaker' pathogenic ataxin-3 (Q77) with or without co-expression of N-VCP. The fly life cycle is outlined above the data and color coordinated with each developmental stage shown in the graph. Means −/+ SD. *p*-values comparing the differences in death at each developmental stage between groups with or without N-VCP were calculated with student's *t*-tests and are shown below the graph. (C) Survival analyses from ubiquitously expressed transgenes in flies throughout development and adulthood. *p*-values: log-rank tests. Black font *p*-value: comparison between "Ctrl" and "Atxn3 (Q77) + N-VCP" groups. Red font *p*-value: comparison between "Atxn3(Q77)

Author Manuscript Author Manuscript Author Manuscript Author Manuscript

+ N-VCP" and "Atxn3(Q77) without N-VCP" groups. (D) Survival analyses from pan-neuronally expressed transgenes in flies throughout development and adulthood. *p*-value: log-rank test. (E) Survival analyses from pan-neuronally expressed transgenes in adult flies only. We utilized an RU486-dependent elav-GS-Gal4 driver to initiate expression of ataxin-3 and N-VCP transgenes in adults. Flies developed and eclosed in media without RU486 and were introduced to media with RU486 on the day of eclosion and were maintained on media with RU486 for their entire lives. *p*-value: log-rank test.

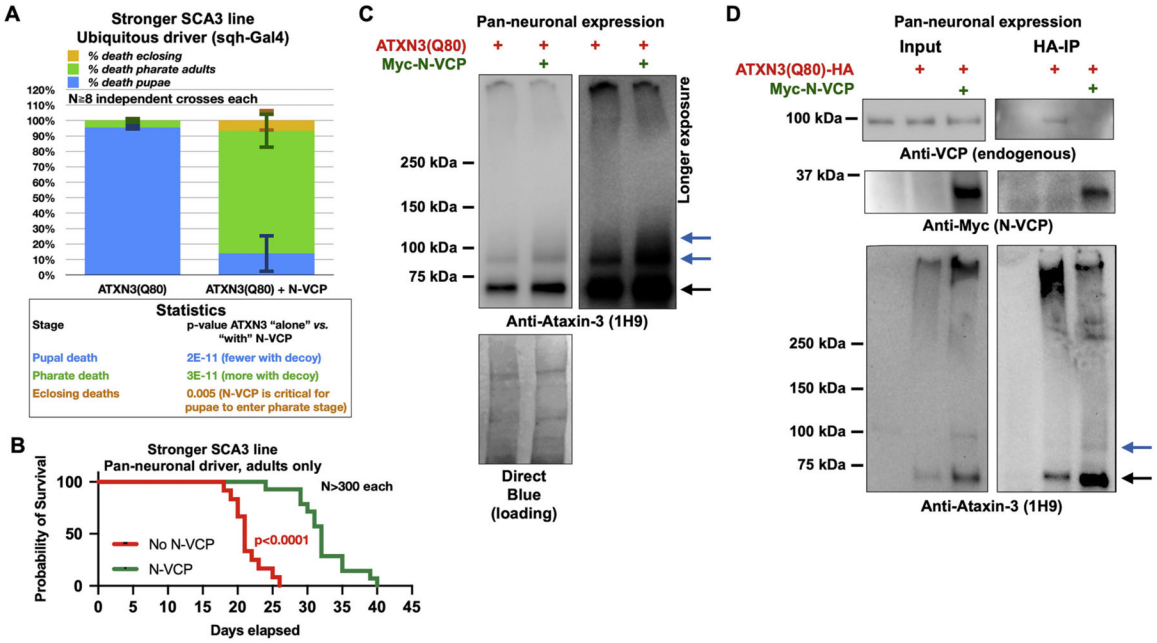


**Fig. 3.**

N-VCP reduces toxicity from pathogenic ataxin-3 with 80Q.

(A) Observations of developmental lethality in flies ubiquitously expressing the 'stronger' pathogenic ataxin-3 (Q80) with or without N-VCP. Means −/+ SD. *p*-values below graph: student's t-tests. (B) Survival analyses from adult-only pan-neuronally expressed transgenes. *p*-value: log-rank test. (C) Western blots of lysates from whole flies pan-neuronally expressing the 'stronger' pathogenic ataxin-3 alone or with Myc-tagged N-VCP. Black arrow: main, unmodified ataxin-3 band. Blue arrows: ubiquitinated species of ataxin-3. (D) Co-immunopurification using whole fly lysates expressing the noted transgenes.



Author Manuscript Author Manuscript Author Manuscript Author Manuscript

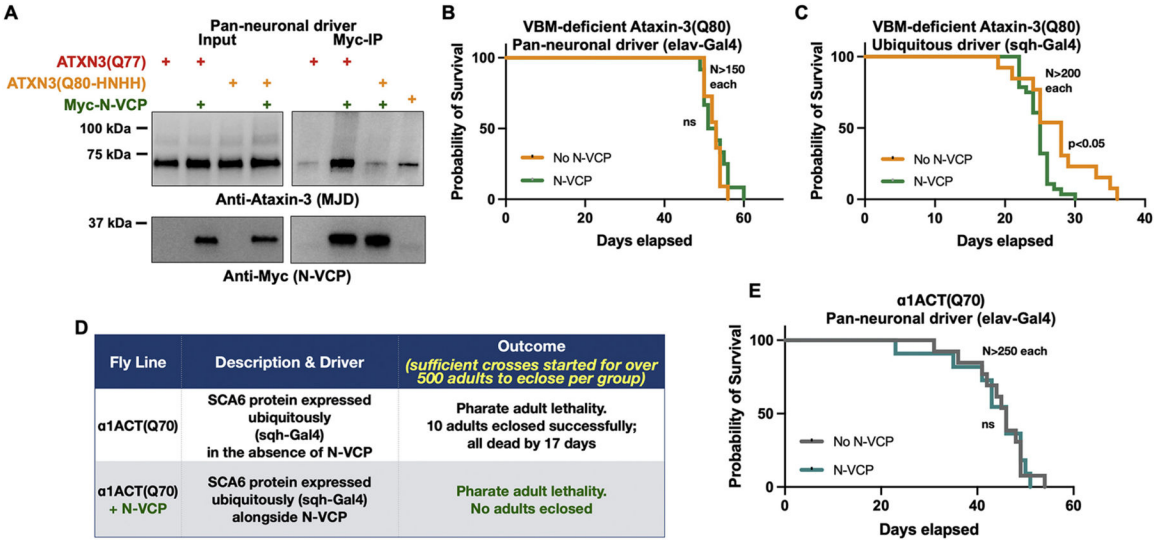


**Fig. 4.**

The ameliorative effects of N-VCP are specific to ataxin-3 and require its intact VBM. (A) Co-immunopurification assays of whole fly lysates expressing one of two forms of ataxin-3: pathogenic ataxin-3 Q77 or pathogenic ataxin-3 Q80 with a mutated VBM ('RKRR' to 'HNHH') without or with N-VCP. (B) Survival analyses of flies pan-neuronally expressing VBM-mutated, pathogenic ataxin-3 with or without N-VCP. Statistics: log-rank test. (C) Survival analyses of flies ubiquitously expressing pathogenic, VBM-mutated ataxin-3 with or without VCP. *p*-value: log-rank test. (D) Summary of transgenes and outcomes of their expression. (E) Survival analyses of flies pan-neuronally expressing α1ACT(Q70) with or without VCP. Statistics: log-rank test. "ns": non-statistically significant.



Author Manuscript Author Manuscript Author Manuscript Author Manuscript

Author Manuscript Author Manuscript Author Manuscript Author Manuscript

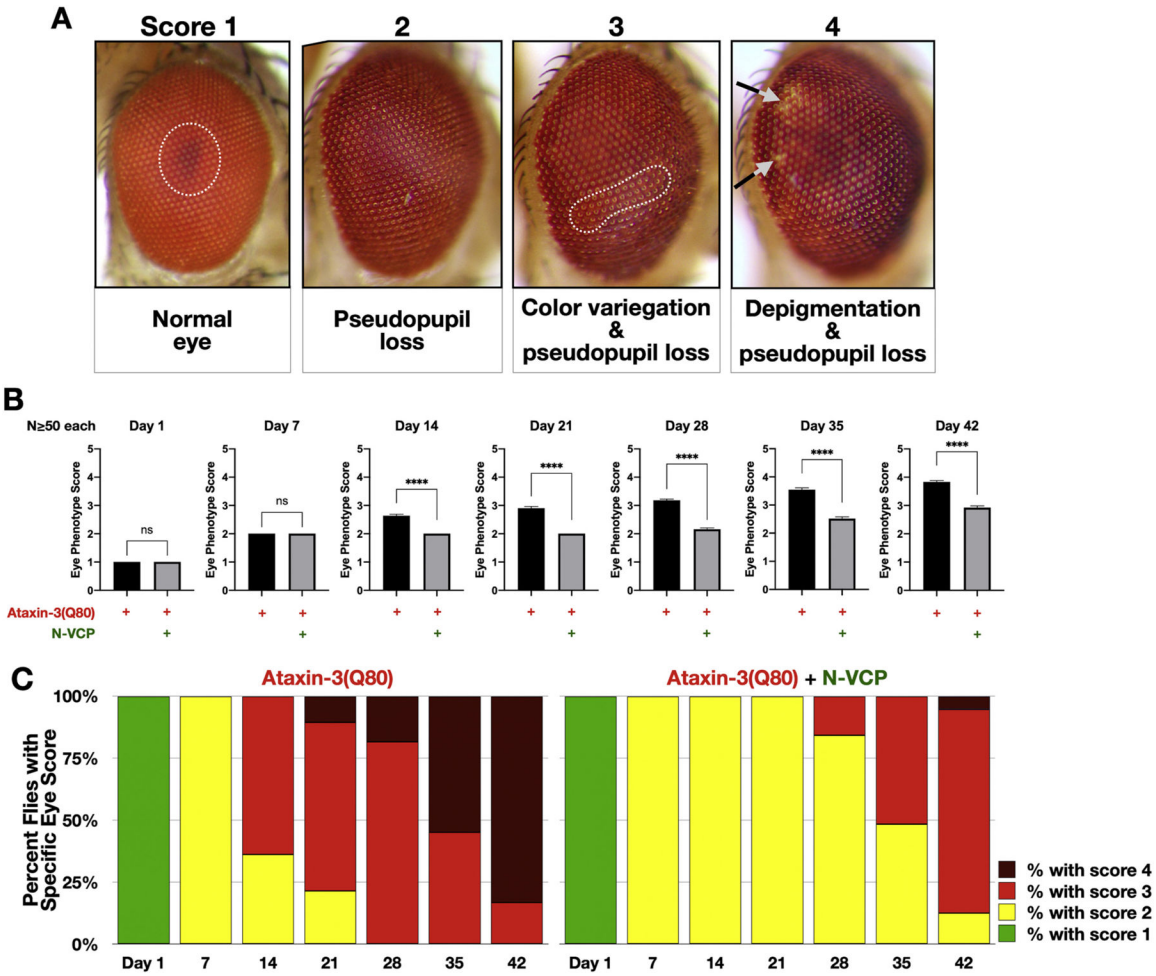


**Fig. 5.**

N-VCP improves pathogenic ataxin-3 toxicity in fly eyes.

(A) Scoring scale and representative images. Distinguishing features from each score category are highlighted. 1) Normal (wild-type-looking) eye; 2) Loss of the pseudopupil; 3) Early signs of color variegation in addition to pseudopupil loss; 4) Depigmentation of a portion of the eye in addition to color variegation and pseudopupil loss. (B) Average eye score in each group at each time point. Statistics: Mann-Whitney tests comparing eye scores at each time point between those expressing pathogenic ataxin-3 alone or with co-expression of N-VCP. Shown are means -/+ SEM. *p*-value: **** = 0.0001. “ns”: non-statistically significant. (C) Representation of the dispersion of eye scores at each time point for each group from (B).

Author Manuscript Author Manuscript Author Manuscript Author Manuscript

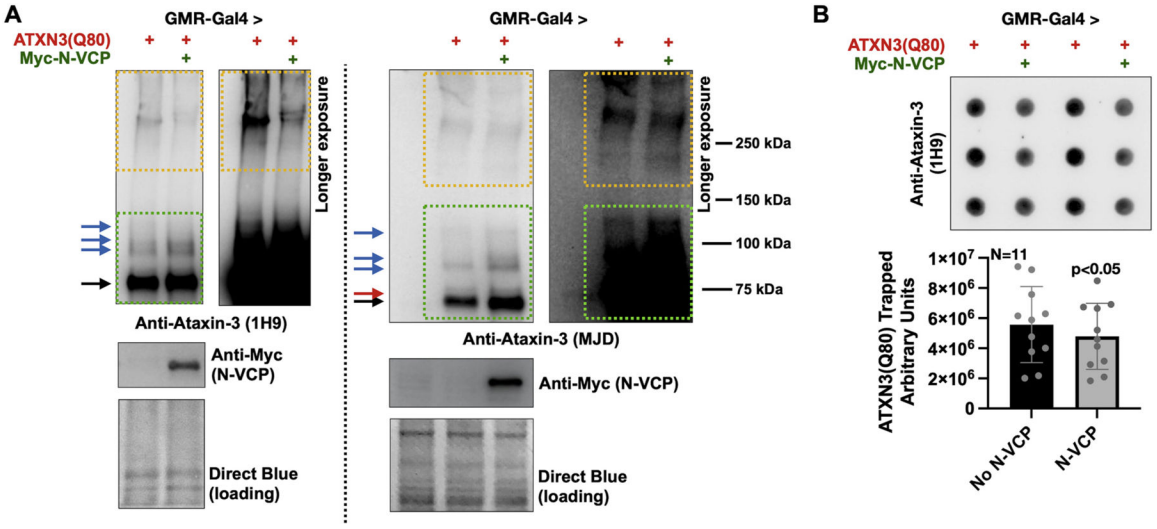


**Fig. 6.**

N-VCP reduces pathogenic ataxin-3 aggregation.

(A) Western blots of lysates from dissected fly heads expressing pathogenic ataxin-3 with or without N-VCP in fly eyes. Orange outlines: SDS-resistant ataxin-3; green outlines: SDS-soluble ataxin-3. Black arrow: unmodified ataxin-3. Red arrow: potentially phosphorylated form of ataxin-3. Blue arrows: ubiquitinated forms of ataxin-3. (B) Filter-trap assays of lysates from the same fly lines as (A). Means -/+ SD, arbitrary units representing intensity of ataxin-3 signal. *p*-value: two-tailed, student's t-test.

Author Manuscript Author Manuscript Author Manuscript Author Manuscript

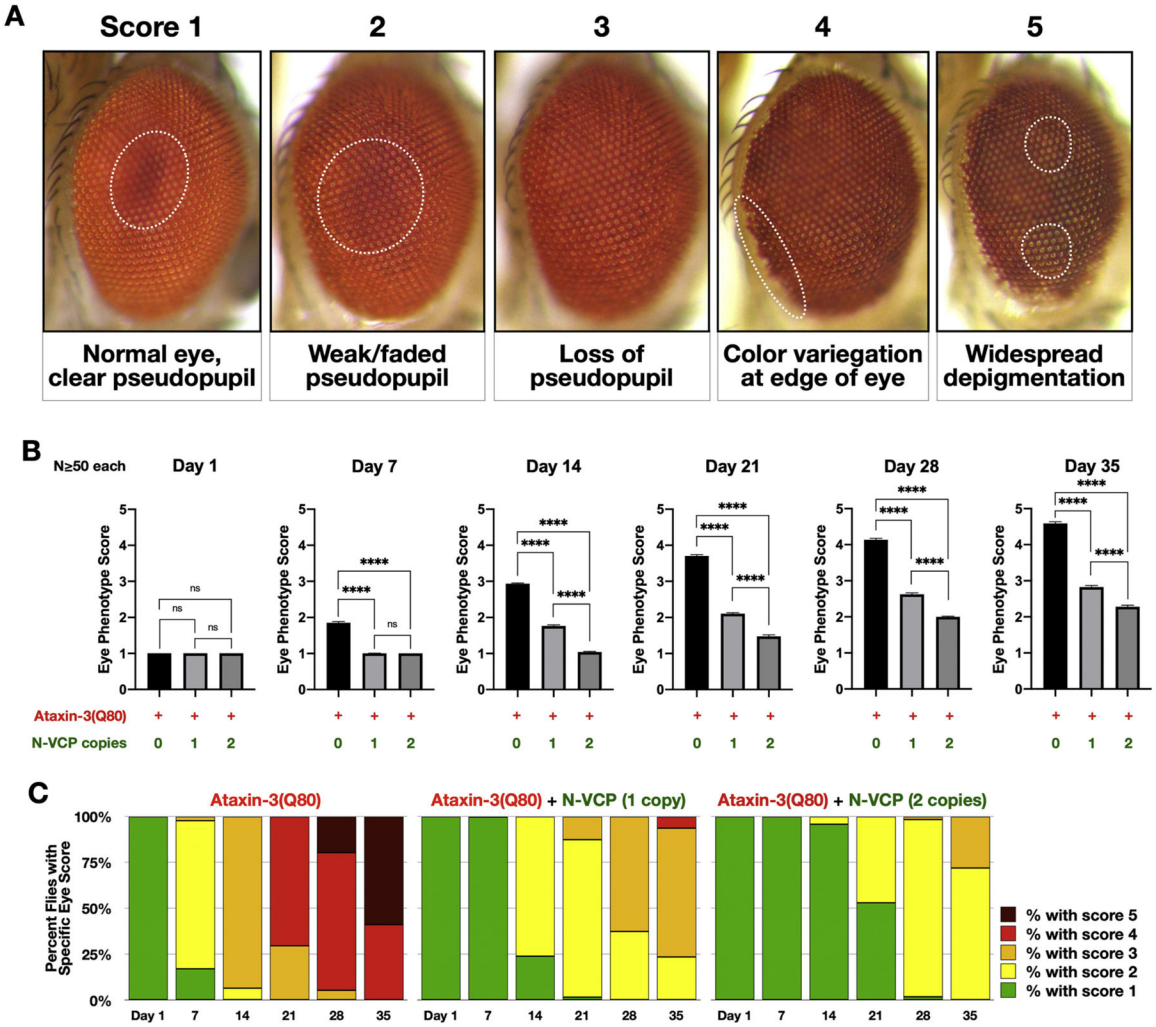


**Fig. 7.**

Dose-dependent N-VCP alleviation of pathogenic ataxin-3 toxicity in fly eyes.

(A) Expanded scale of representative images for eye scoring system. Distinguishing features from each score category are highlighted. Scoring system is as follows: 1) Normal (wild-type-looking) eye with a clearly defined pseudopupil; 2) Weaker pseudopupil that has begun to fade; 3) Undetectable pseudopupil; 4) Color variegation at the edge of the eye in addition to pseudopupil loss; 5) Widerspread depigmentation in addition to color variegation and pseudopupil loss. (B) Average eye score for each group at each time point. Shown are means -/+ SEM. Statistics: Kruskal-Wallis and Dunn's multiple comparison tests comparing all three groups. *p*-value: **** = 0.0001."ns": non-statistically significant. (C) Representation of the distribution of eye scores for each group at each time point.

Author Manuscript Author Manuscript Author Manuscript Author Manuscript

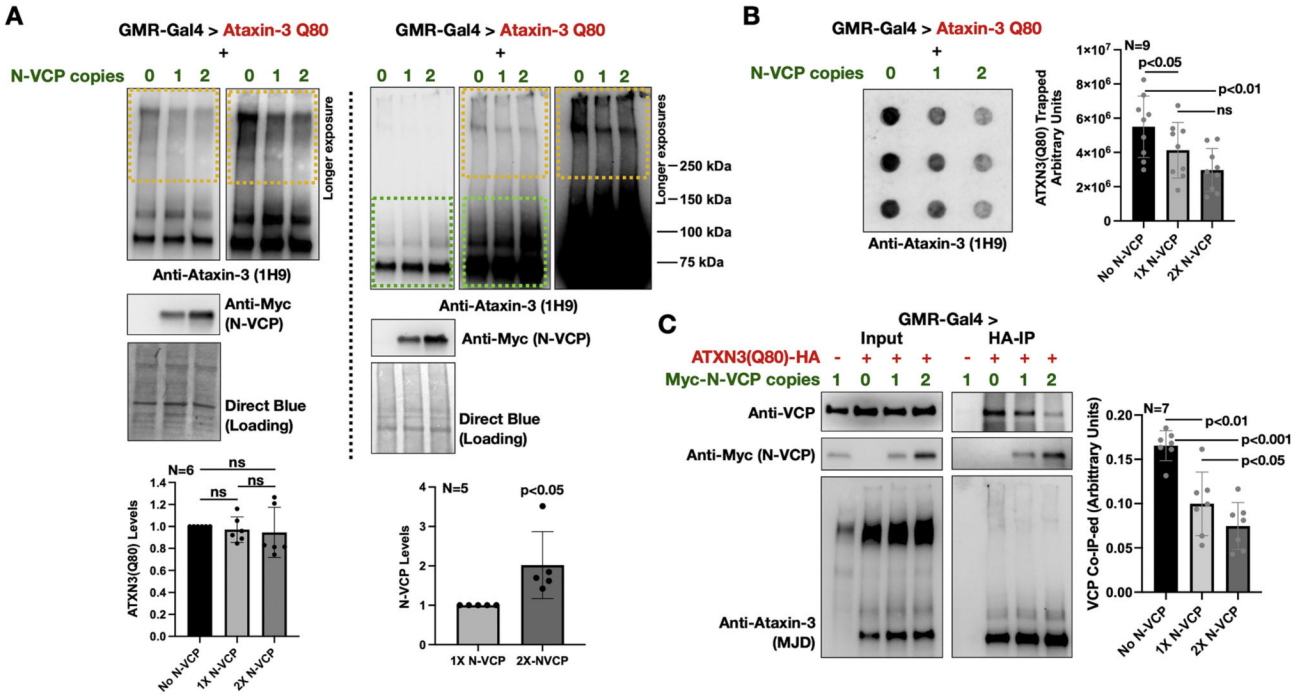


**Fig. 8.**

N-VCP dose-dependent reduction of ataxin-3 aggregation and inhibition of interaction with VCP.

(A) Western blots of lysates from dissected fly heads expressing pathogenic ataxin-3 alone, or with one or two copies of the N-VCP transgene in fly eyes. Two biological repeats are shown. Quantifications: Means -/+ SD, normalized to ataxin-3 without N-VCP (ataxin-3 graph), or normalized to one copy of N-VCP (N-VCP graph). Statistics: one-way ANOVA with Tukey's multiple comparisons test to compare ataxin-3 protein levels, and student's t-test to compare N-VCP levels. Orange outlines: SDS-resistant ataxin-3; green outlines: SDS-soluble ataxin-3. (B) Filter-trap assays of lysates from the same crosses as in (A). Means -/+ SD, arbitrary units representing intensity of ataxin-3 signal. *p*-value: repeated-measures one-way ANOVA with Geisser-Greenhouse correction and Tukey's multiple comparisons test. (C) Co-immunopurification assays using bead-bound anti-HA antibody. Statistics: one-way ANOVA with Tukey's multiple comparisons test. Means -/+ SD. "ns": non-statistically significant.

Author Manuscript Author Manuscript Author Manuscript Author Manuscript

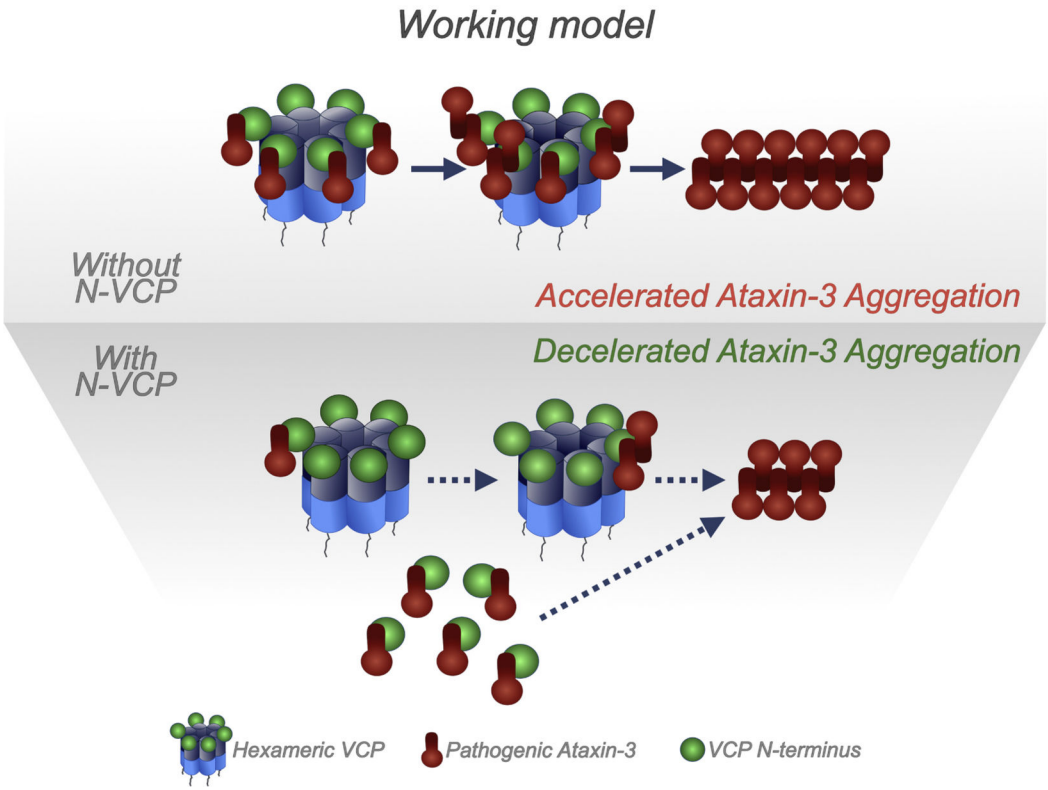


**Fig. 9.**

Model of N-VCP-dependent benefits.

Upper panel: Endogenous VCP hexamers may bind multiple pathogenic ataxin-3 proteins, bringing them into closer physical proximity and accelerating their aggregation. Lower panel: Pathogenic ataxin-3 is bound by N-VCP, disrupting its interaction with VCP hexamers, preventing the seeding effect.